Journal of Mechanical Engineering and Sciences
ISSN (Print): 2289-4659; e-ISSN: 2231-8380
Volume 13, Issue 3, pp. 5665-5688, September 2019

DOI: https://doi.org/10.15282/jmes.13.3.2019.28.0454

Performance analysis of multi-row vertical axis hydrokinetic turbine–straight blade cascaded (VAHT-SBC) turbines array

E. Septyaningrum[1*], R. Hantoro[1], I. K. A. P. Utama[2], J. Prananda[3], G. Nugroho[1], A. W. Mahmashani[1], N. A Satwika[1]

[1]Department of Engineering Physics, Institut Teknologi Sepuluh Nopember
Surabaya, Indonesia
[*]Email: erna.septya@gmail.com
Phone: +62857 4149 3003
[2]Department of Naval Architecture, Institut Teknologi Sepuluh Nopember
Surabaya, Indonesia
[3]Department of Naval Engineering, Institut Teknologi Sepuluh Nopember
Surabaya, Indonesia

ABSTRACT

Due to its high energy concentration, hydrokinetic energy from tidal and rivers flow provides great expectation. One of the effective ways to meet the energy production target is to reduce the installation and maintenance effort by arranging turbines in such configuration, known as hydrokinetic turbine array. The performance of array configuration is affected by turbine position and rotational direction. Thus, research on this issue is needed to get a turbine array configuration design with optimum performance. This work provides a comprehensive analysis of the effect of turbine rotational direction and position on the array performance. To achieve this objective, the experimental study and URANS based CFD (Computational Fluid Dynamic) simulation were carried out. This study proposed 3 side-by-side configurations, and 2 multi-row configurations, i.e. 3T-A and 3T-B. The side-by-side configuration consists of Co-rotating (Co), counter-rotating-in (CtI) and counter-rotating-out (CtO). While the multi-row configuration consists of 3T-A and 3T-B. The comprehensive information is provided. Both experimental and numerical study confirmed that the velocity superposition in the interaction zone gives a constructive effect on turbine performance. Hence, all site-by-site configurations are able to enhance farm effectiveness approximately 30% at an incoming flow velocity of 1.3 m/s. However, Co configuration is recommended to be installed in the resource having unpredictable flow direction, since its performance is independent to the incoming flow direction. Meanwhile, the CtI is suitable for canal or river since it has better performance for unidirectional incoming flow. The study for multi-row configuration shows the effect of upstream turbines to the downstream turbine. The 3-TA configuration has better performance than 3T-B, because side-by-side configuration installation as the upstream turbine could compensate for the bad effect of upstream turbine wake.

Keywords: Array; counter-rotating; farm-effectiveness; hydrokinetic; multi-row.

INTRODUCTION

The decreasing fossil fuel reserve leads to the growth of renewable energy. Shifting to renewable energy ensure for reliable and cost-effective delivery of energy without the environmental threat. Renewable energy could be relied on to comply with energy needs for the rural area. For this purpose, the hydrokinetic energy conversion system is widely developed. Due to its high energy concentration and predictability, hydrokinetic energy from tidal and rivers flow provides great expectation [1].

Along with Indonesia's development, energy demands have increased rapidly. More than 80% of energy needs in Indonesia are supplied from fossil fuel, which the reserves are continuously decreasing. Therefore, renewable energy resources are urgently required to reduce dependence on fossil fuels. One of the promising resources is hydro energy. Implementation of hydro energy conversion system in Indonesia provides a promising opportunity, considering its potency in 45.379 MW [2]. The hydrokinetic turbine is suitable for the future need of Indonesia since the technology is proven. Moreover, it easy to be implemented and maintained. In accordance with it, Indonesia develops hydrokinetic energy, since it is one of the priority research topics released by the Ministry of Research, Technology and Higher Education. The Indonesian Government supports the expansion of hydrokinetic technology through many policies.

The application of Vertical Axis Hydrokinetic Turbine (VAHT) seems to be the promising technology for that purpose since it could generate power under low current speed, omnidirectional (independent of current direction), unrequired of yaw mechanism and easy to maintenance [3]–[6]. Unfortunately, the efficiency and the self-starting ability of VAHT is deficient [4]. Hence intensive research has been stimulated to overcome this issue through the design modification and components addition for VAHT [6]–[11]. Previous research had proposed the novel design of Vertical Axis Hydrokinetic Turbine -Straight Blade Cascaded (VAHT-SBC) [12]. The engagement of passive pitch mechanism and cascaded blade is proven to enhance the efficiency and self-starting ability of turbine [13]–[15]. The VAHT-SBC with 9 blades has efficiency of 0.42, which is closed to the theoretical Cp for VAHTs (0.45) [12].

To meet the energy production target and reduce the installation and maintenance effort, the turbine was installed in such configuration, known as the hydrokinetic turbines array. Currently, the industry moves from single demonstrator project to array project, e.g. My Gen project site in 2016. My Gen has been continently developed and installed 4 turbines to generate electricity. It has been predicted that the development of the turbines array would increasingly grow in 2020 [16]. Some of the other hydrokinetic turbine projects are Gen5 KHPS 35 kW (USA); AR1500 1.5 MW (Singapore); SeaGen 1.2 MW (England); SR250 250 kW(Scotland); Cormat 250 kW (Scotland); TREK 340 kW (Canada); Open-Center Turbine 300 kW (Ireland); TidGen 150 kW (USA) and so on [17]. The SeaGen design was the world's first commercial-scale tidal turbine. Meanwhile, the development of hydrokinetic turbines in Indonesia is still not widely implemented, even though Indonesia has considerable hydrokinetic energy potential, both inland (rivers) and ocean currents.

Due to the high cost and complex operational, it is required a good understanding method for turbines array installation. A comprehensive study is needed to analyze the complex flow and the interaction of turbines on an array. Information about weak characteristics and hydrodynamics interaction between turbines is very important [18]. These

are the main consideration for designing array, both for wind turbines array and hydrokinetic turbines array. Many works analyze the effect of turbine position within array using theoretical, experimental and/or computational methods. Research conducted by [19] confirmed that the lowest turbine separation provides the highest power output. Meanwhile, [20] quantified the performance of two turbines which interacting with each other in an array. This study focuses on the power and thrust measurement.

Comprehensive knowledge regarding the flow around the turbines is needed for designing an array. Due to the energy extraction process, the complex flow appears around the turbine, which is characterized by the formation of turbulent flow with large vortices. The high value of vorticity indicates that there are many vortices. The vortices have rotating flow direction, which greatly affects the formation of hydrodynamic force on a blade. One of the quantities that used for representing turbulence level is turbulent intensity, as given in Equation 1 [16].

$$\text{Turbulent intensity } \mathrm{I} = \frac{\sqrt{\frac{1}{3}(u'^2 + v'^2 + w'^2}}{U_o} \tag{1}$$

Since the turbulence thickens the boundary layer, it could increase the drag. It also postpones the stall hence the optimal lift formation could be achieved.

Studies have been conducted to determine the characteristics of flow around the turbine, both numerically and experimentally. Some studies employed actuator disc approximation methods to investigate the characteristics of turbine and array turbine [21]–[24]. However, the various simplifications used in the actuator disc approximation method make this theory unable to flow around the blade and only reduce the momentum across the disc [22]. This is supported by a research conducted by [21] which shows that vortex shedding from the disc lacks swirls production flow.

Research [25] carried out an experiment to determine the flow characteristics around the horizontal axis turbine and clarified that the fluid flow in the wake area has opposite directions to the direction of rotation of the turbine. This research was then continued by [26] who conducted an experimental study to analyze the effect of downstream turbine rotation on its performance. This study shows that while the downstream turbine and the upstream turbine rotate in difference direction, the performance of downstream turbine increases. The installation of counter-rotating turbines in the downstream zone could increase the farm effectiveness [27].

The existence of upstream and downstream blades on the vertical axis turbine (VAT) leads more complex flow than the horizontal axis turbine (HAT). Therefore, not all HAT concepts could be applied directly to VAT because it could cause incompatibility of phenomena and models for analysis and design [28], [29]. However, the phenomenon of different rotational direction between flow around the turbine and the turbine itself appears both types of turbines. Research conducted by [30] shows that cross-stream velocity in the leeward region has a negative sign and the windward site has positive sign, which indicates that the vortex is in the windward region and leeward rotates in the different direction. When the VAT rotates, two pairs of counter-rotating vortices exist, which have a rotating direction opposite the direction of the turbine rotation [31]. Therefore, a comprehensive analysis of the effect of turbine rotation direction on turbine array performance is needed.

The previous studies clearly show that the turbine position and rotational direction affect the array performance. However, most of these is for Horizontal Axis Wind Turbine

(HAWT). The research which is carried out for Vertical Axis Hydrokinetic Turbine (VAHT) array is very rare, although the hydrodynamic interaction in the VAT array are more complex that HAT array. Moreover, the different characteristic of air and water might lead to a difference effect on turbine performance. The currently work provide analysis of turbine rotational direction toward farm effectiveness of VAHT array. It tries to present a comprehensive analysis regarding to the effect of turbine rotational direction on hydrokinetic turbines array performance. It also proposed multi-row hydrokinetic turbine to optimize energy harvesting process. Multi-row arrays were designed by considering the phenomenon appears in the side-by-side configuration. The analysis that would be presented is emphasized on differences in flow interactions due to turbine rotational direction, including the velocity and turbulent intensity around turbines. This currently work is a continuation of the previous research that have succeeded in designing VAHT-SBC. The result not only for the basis of VAHT-SBC array design, but also for all type of VAHT array.

EXPERIMENTAL AND NUMERICAL SIMULATION APPROACH

Experimental Study

An experimental study was carried out at a towing tank, Hydrodynamic Laboratory, Institut Teknologi Sepuluh Nopember. This facility has the working section of 50 m length, 3 m width and 2 m water depth. The turbine design was adopted from the previous study [13] which is known as VAHT-SBC, given in Figure 1. The blades of VAHT-SBC are made of NACA 0018 hydrofoil. The blades are made of fibbers, resin and reinforcement iron in the middle of the blade. The arms are made of solid iron which is strength enough to withstand the moment of great inertia during the turbine rotation. The shaft is also made of solid iron, which is tapped, so the top end diameter is longer than the bottom. The reason is to minimize the drag at the bottom end of the shaft and avoid shaft bending. The turbine is on overhanging position, hold by using clamp F. The installation of clamp F must be robust enough, thus the turbine would not be shaky and endanger the turbine structure.

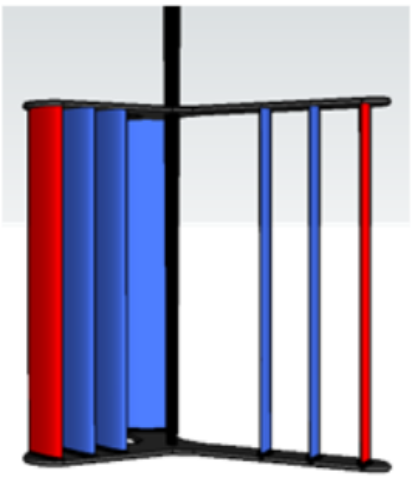

Figure 1. Vertical Axis Hydrokinetic Turbine – Straight Blade Cascaded. The blue blades are fix blade, and the red blades are passive pitch blades.

Figure 2 shows the experimental setup for side-by-side turbines configuration. Turbines were hung on the cart, which is located above the towing tank. All blades and arms of the turbine were submerged in the water, while the frame and the bearing system were above the water surface. The velocity of the cart was controlled from the control room by operator. To reach the desired velocity, the cart would experience acceleration first, until it finally reaches a stable velocity in accordance with set point. Data retrieval was still done during the cart was move. However, data that will be identified and used to analyse the array performance was data obtained when the cart reach its stable velocity. The velocity variation being presented here are 0.7 m/s; 1 m/s and 1.3 m/s. Identification of turbine RPM is obtained by the video recording from cameras which is mounted straight on the turbines, aiming to make a good quality video and obtained accurate data. A tachometer was also used as the validators for data obtained from video recording. The validation shows that the difference between tachometer's data and video recording's data is 3%. The RPM data was obtained from the experimental study and used as input data in the numerical simulation study.

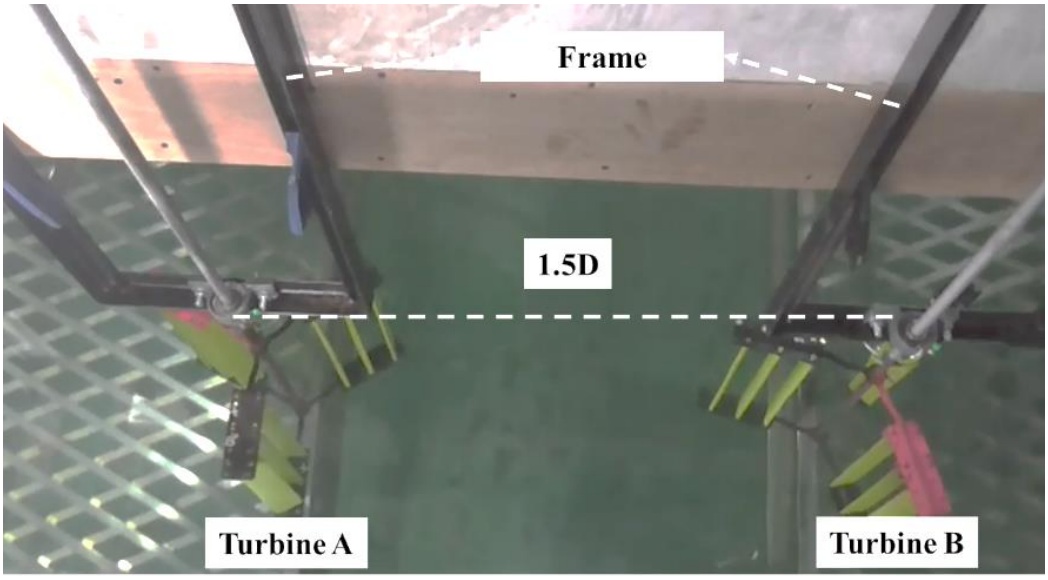

Figure 2. Turbines installation in the cart (obtained from a camera located straight above the turbines)

The utilization of a towing tank for turbine testing is one of the recommended methods due to its controlled flow condition. The turbine testing causes unstable and asymmetric flow. The blockage effect should be taken into account as it affects turbine performance. Mathematically, the blockage ratio is formulated in Equation (2) [32].

$$B = \frac{1}{4}\left(\frac{A_{turbines}}{A_{towing\_tank}}\right) \tag{2}$$

$A_{turbines}$ is turbine cross-section area and A_{towing_tank} is towing tank cross-section area. Refers to [33], there is no correction of the turbine output for the blockage ratio less than 5%. All configurations in this study have a blockage ratio of approximately 1.33%, hence there is no need for correction of the torque value as a consequence of the blockage effect.

The first step of this study is stand-alone turbine performance testing. The performance of the stand-alone turbine is used as the comparison to calculate the farm effectiveness (ε_{farm}). The power produced by the stand-alone turbine is approximately 4.17 – 29.39 W at velocity variation of 0.7 – 1.3 m/s. The Cp of the stand-alone turbine seems to be low due to the low turbulent intensity. It is about 0.15 – 0.17. Since the TSR of the turbine is low, mostly it has low Cp. At that conditions, the turbine could generate torque, which is enough to rotate the turbines itself, but in poor rotational velocity. This condition indicates that some blades are in stall condition, which has more powerful drag than the lift force, hence the energy extraction process is not optimal.

After standalone turbine testing, the turbine array is then tested to identify the array performance. The performance of hydrokinetic turbines arrays is represented by farm effectiveness, then other work uses the term of farm efficiency. Farm effectiveness expresses the array's ability to convert the hydrodynamic energy in channel or river. The farm effectiveness expresses the proportion of channel potency which could be extracted by the turbines. It shows the effectiveness of the array in exploiting the potential of the channel [34]. Research conducted by [35] state that the farm effectiveness is the ratio between the power produced by farm and the power generated by N Isolated turbines, where N is the number of turbines in the farm, mathematically described in Equation (3)-(5). The isolated turbine is also known as the stand-alone turbine.

$$\varepsilon_{farm} = \frac{P_{farm}}{P_{ref\_farm}} \tag{3}$$

$$P_{farm} = \sum_{i}^{N} P_i \tag{4}$$

$$P_{ref\_farm} = N.P_s \tag{5}$$

P_{farm} is the total power generated by the array and P_s is the power generated by the stand-alone turbine. Whereas the $P_{ref\ farm}$ does not only indicate the power produced by the stand-alone turbine, but also the power when there is no hydrodynamics interaction.

Three design of side-by-side turbine array configuration was tested in this work, i.e. "Co-rotating configuration" (Co), "counter-rotating-in configuration" (CtI) and "counter-rotating-out configuration" (CtO), as depicted in Figure 3. They are distinguished from their rotational direction. The first configuration known as co-rotating configuration (Co) arranges form identical turbines in the same rotational direction, while the others arrange 2 turbines with different rotational direction, known as "counter-rotating in" (CtI) Configuration and "counter-rotating out" (CtO) Configuration.

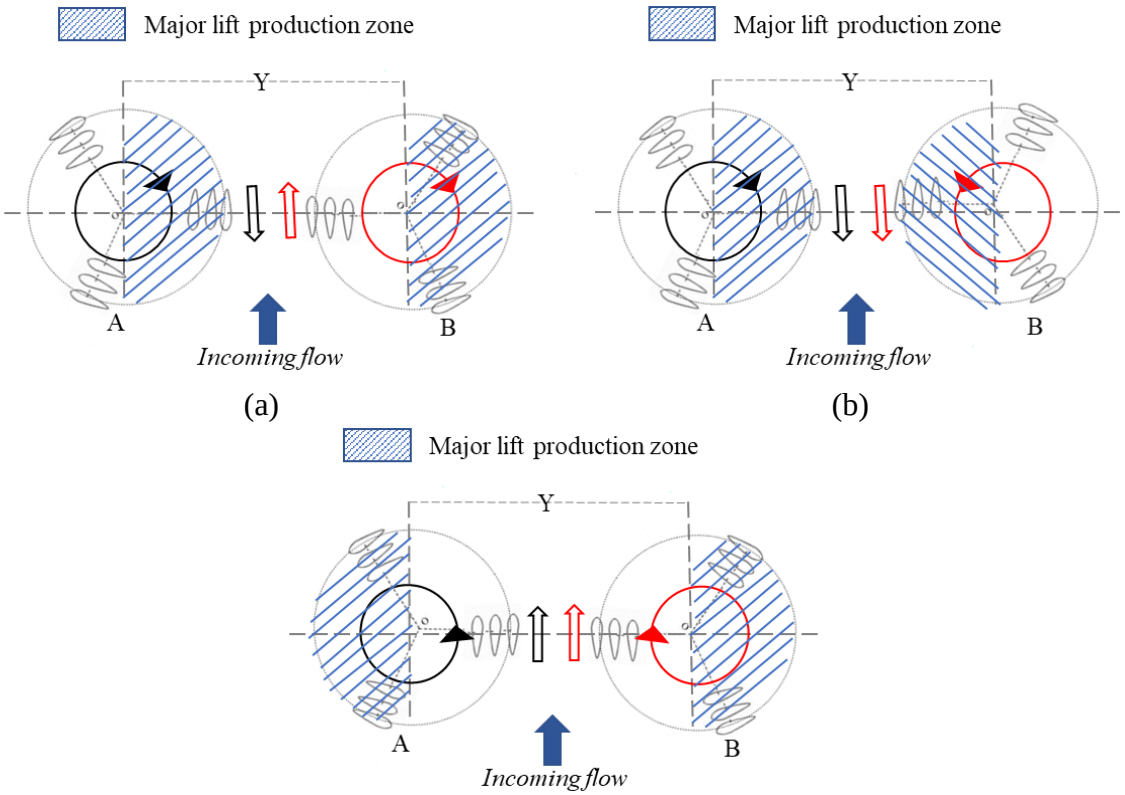

Figure 3. The position of major lift production zone for (a) Co configuration, (b) CtO configuration, (c) CtI configuration

Based on the result of site-by-side configuration testing, this work also proposed two multi-row array turbine configurations, illustrated in Figure 4. The configurations called 3TA and 3TB. The downstream distance between first and the second row is 3D, where D is turbine diameter.

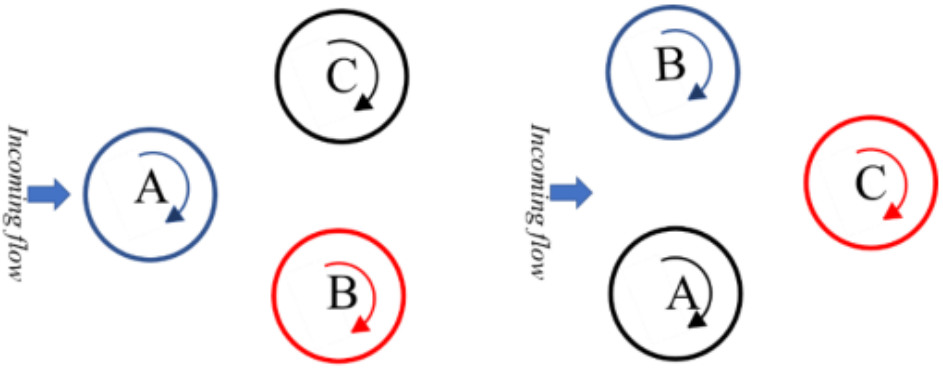

Figure 4. Multi-Row Configuration; a. 3TA configuration; b. 3TB configuration

Numerical Simulation Study

A 2D Unsteady Reynold Average Navier-Stoke (URANS) Computational Fluid Dynamic Simulation was conducted in this work, using ANSYS FLUENT. The numerical study aims to get complementary data for detail information. Due to the limitation data and the high cost of the experimental study, numerical simulation seems to be a promising method to get more complete information. The numerical simulation consists of 3 main steps, i.e. pre-processing (geometry, mesh generation and setting), processing (solver) and post-processing (result).

This work used 2D URANS simulation, which is employed since it capable to clarify the influence of large-scale flow unsteadiness [36]. URANS simulation has been successfully solving the problem with deterministic unsteadiness, such as vortex shedding in the wake of a two-dimensional obstacle with a low-turbulence approach flow [37]–[42]. The difference between Reynold Average Navier-Stoke (RANS) and URANS is that the addition of unsteady term which is present in the URANS momentum equation [43]. URANS approach is mathematically expressed in the Equations (6) and (7).

$$\frac{\partial U_i}{\partial x_i} = 0 \tag{6}$$

$$\frac{\partial U_i}{\partial t} + U_j \frac{\partial U_i}{\partial x_j} = -\frac{1}{\rho}\frac{\partial p}{\partial x_i} + \frac{\partial}{\partial x_j}\left[v\left(\frac{\partial U_i}{\partial x_j} + \frac{\partial U_j}{\partial x_i} \right) - \overline{u_i' u_j'} \right] \tag{7}$$

Where t and x_i is the time and space cartesian coordinates, U_i and u_i' are the time-averaged and fluctuating flow velocity component. P is the time-averaged pressure, ρ and v are the fluid density and the kinematic viscosity respectively. The Reynold stress tensor $\overline{u_i' u_j'}$ is an unknown component that has to be modeled.

The *k-ω* STT model was utilized as the turbulence model. *K-ω* STT suitable turbulence model in solving cases with adverse pressure gradients and high flow separations. This turbulence model is widely used for simulation of hydro turbines and wind turbines[4], [13], [44]–[47]. *k-ω STT* is the combination of two turbulence model [48], i.e. the Wilcox *k-ω* is retained for the near wall region and the *k-ε* model is kept in the fully turbulent region far from the wall due to the free-stream independence [49]. The *k-ω STT* model is two-equation model, i.e. *k* for the specific turbulent kinetic energy and *ω* for the specific dissipation rate (or specific turbulent frequency), as given in Equations (8) and (9) respectively [50].

$$\frac{\partial(\rho k)}{\partial t} + \frac{\partial}{\partial x_i}(U_i \rho k) = \frac{\partial}{\partial x_j}\left(\mu_k \frac{\partial}{\partial x_j} k \right) + \bar{P}_k - \beta^* \rho \omega k \tag{8}$$

$$\frac{\partial}{\partial t}(\rho\omega) + \frac{\partial}{\partial x_i}(U_i \rho \omega) = \frac{\partial}{\partial x_j}\left(\mu_k \frac{\partial}{\partial x_j} \omega \right) + \bar{P}_\omega - \beta^* \rho \omega^2 + 2\rho(1-F_1)\frac{1}{\omega}\frac{1}{\sigma_{\omega,2}}\frac{\partial}{\partial x_j} k \frac{\partial}{\partial x_j}\omega \tag{9}$$

Where μ is dynamic viscosity, $\bar{P}$ is the effective rate of production of *k*, $\beta^*$is turbulence modeling constant, F_1 is blending function and $\sigma_{\omega,2}$ is turbulence modeling constant. Other boundary conditions are depicted in Figure 5. The velocity inlet was used because of the use of incoming flow velocity as the input parameter. Meanwhile, the outlet section is set as a pressure outlet. The choice of boundary conditions is also based on literature [51], [52].

The first step of the numerical simulation is to make 2-dimension geometry and generate grid (meshing proses). The geometry knows as simulation domain, should be

representing the actual experimental condition. Two type of domain was used, i.e. the rotational domain and stationary domain, as depicted in Figure 5. The stationary domain is 15D x 3 meters, D is the turbine diameter. The turbine is located 5D from the inlet [52], [53] . The next step is grid generation or meshing. The gird generation process has significant influences on computational results and computation time. Therefore, grid independent studies are needed to determine the optimal grid. The grid independent study was tabulated in Table 1. Based on this table, this work used grid with body size of 5.00E-03 m and the total element is 143712. Grid refinement is needed at certain edge, hence the grid for each domain has a different size. Because rotating domains and turbine parts are very important, these two parts have a smaller grid size. To refine the quality of the grid on the turbines, the inflation technique is used in the turbine wall, shown in Figure 6. The inflation is generated using First Layer Thickness Method, with the value of $1.4x10^{-2}$ mm and maximum number of layers 20.

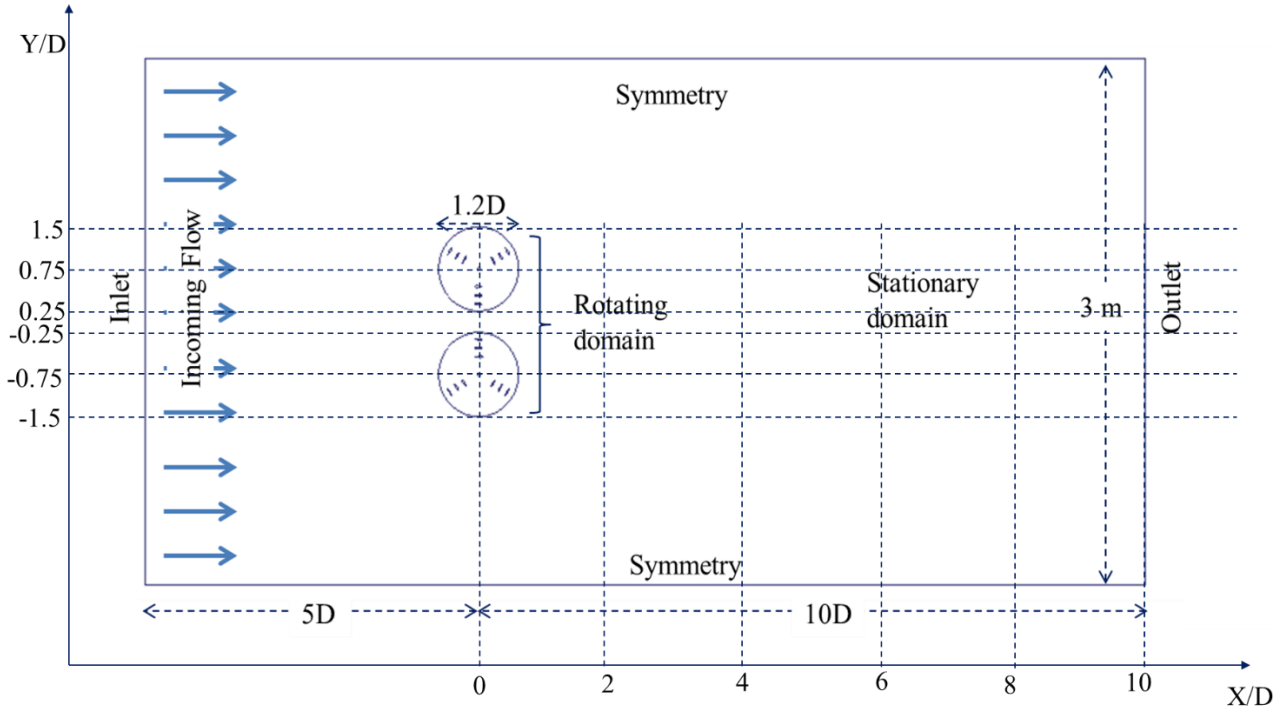

Figure 5. Simulation Domain and Boundary Condition

Table 1. Grid independence study

Grid Size	Number of Element	Orthogonality	Average velocity at 0.4D behind turbines
5.00E-02	129698	0.936	1.0340
7.00E-03	134390	0.938	1.1530
5.00E-03	143712	0.939	1.1950
3.00E-03	188279	0.947	1.1951

The next step is boundary condition setting which is based on the experimental study. The inlet of the domain is defined at velocity inlet, which is varied by 0.7; 1 and 1.3 m/s. The turbine domain is rotating domain which have rpm according to the experimental result. The outlet is set to be pressure outlet. The boundary condition setup was defined in Figure 5. Determination of settings is also based on some literature that conducts similar studies. Table 2 shows a comparison of the settings applied in this work and in previous studies.

Table 2. Literature study for determining numerical simulation parameter

PARAMETER	CURRENT WORK	HANTORO [12]	ZHAO GUANG [52]	ABDOLRAHIM [54]
DOMAIN	- Stationary - Rotating	- Stationary - Rotating	- Stationary - Rotating	- Stationary - Rotating
ROTATING DOMAIN DIAMETER	1.2 D	1.5 D	1.2 D	1.25 D
MESHING TECHNIQUE	Triangular + Inflation	Tetrahedral	Inflation	Quadrilateral cell + Inflation
TURBULENCE MODEL	k-ω SST	SST	k-ε	4-equation transition SST
BOUNDARY CONDITION				
- INLET	Velocity Inlet	Velocity inlet	Velocity inlet	Velocity inlet
- OUTLET	Pressure Outlet	Opening	Pressure outlet	Pressure outlet
- TURBINE	No slip wall	No slip wall	No slip wall	No slip walls

The validation process was carried out to show the conformity between the simulation and experimental results. The validation compared the experimental and simulation results for 3 incoming flow variations and 2 downstream locations, as shown in Table 3. Table 3 shows that the difference between experimental and simulation is 7%, so the simulation results are valid.

After all conditions had been determined, then the simulation is run to get the desired results. The convergence criteria set up to be 10^{-3}. The simulation was done for 2 turn, for each condition. After the solver was completed, continued by taking the simulation result, i.e. velocity data, pressure data, turbulence intensity data and so on. This data gives us additional information for analyzing the experimental result.

Table 3. Model Validation

Incoming velocity	Experimental		Simulation		Difference		Average Difference
	1D	2D	1D	2D	1D	2D	
0.9	0.6	0.79	0.54	0.84	10%	6%	8%
1.1	0.59	0.9	0.57	0.89	3%	1%	2%
1.3	0.95	1.2	1.1	1.3	16%	8%	12%
TOTAL AVERAGE DIFFERENCE							7%

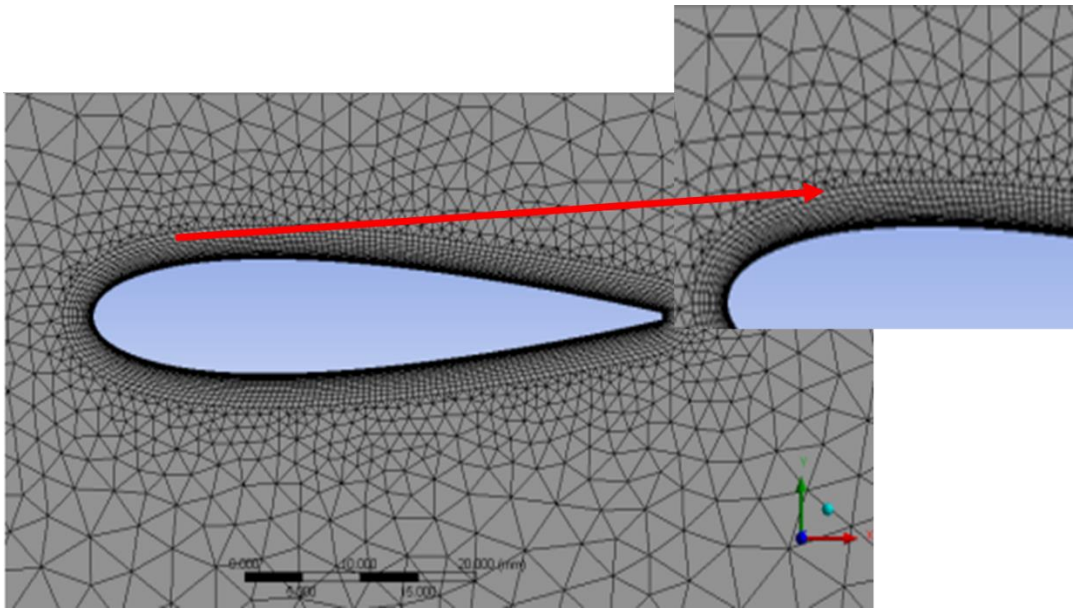

Figure 6. Meshing using inflation technique

RESULTS AND DISCUSSIONS

Performance of Side-by-side Configuration

The hydrokinetic technology is rapidly growing. One of the interesting issues is the optimization of existing resource using turbine arrays. Turbines array is an arrangement of several turbines in a particular configuration. Due to the close distance between turbines, the hydrodynamic interaction within turbine plays an important role in the determination of turbines performance. Hence, it is the major consideration in designing a turbines array.

This study proposed three types of side-by-side turbines configuration which indifferences rotational direction, aiming to determine the effect of turbines rotational direction on the array performance. As the turbines rotate in the different rotational direction, the hydrodynamics interaction exists within the turbines is not the same, influencing the

performance of each turbine. We could clearly distinguish the hydrodynamic interaction from the simulation result. The experimental results confirm that each site-by-site turbine configuration has different performance, since their hydrodynamics interaction is not the same, as depicted in Figure 7. CtI configuration has the best performance than others, especially at low incoming flow velocity, in which the performance of array turbine is represented as the value of farm effectiveness. The farm effectiveness of CtI is approximately 1.19-1.3. Meanwhile, the farm effectiveness for Co and CtO is approximately 1.17 – 1.3 and 0.8 – 1.37, respectively. Almost all designed configurations have the farm effectiveness of more than 1, indicating that hydrodynamic interaction gives the constructive effect. The destructive effect exists on CtO at low TSR (low incoming flow velocity. At this condition, the farm effectiveness of CtO configuration is below 1.

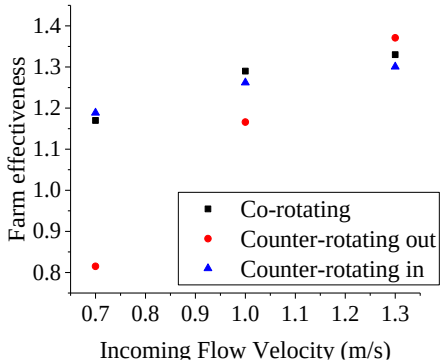

Figure 7. Farm effectiveness for each configuration

Due to limitation of data obtained from the experimental study, the numerical simulation was conducted to get deeper information regarding to the hydrodynamic interaction. Numerical simulation result confirm that the hydrodynamics interaction turns out to give different effects on each turbine. The position of major lift production area toward interaction zone plays important role in determining the performance of turbines. For Co configuration, the Cp of turbine A is better than turbine B, since the major lift production area of turbine A is in the interaction zone. Hence, the constructive effect of hydrodynamics interaction gives more significant impact on turbine performance, as illustrated in Figure 3 (a).

The superposition of induced flow and the incoming flow determine the strength of flow in the interaction zone [32][55]. Because both induced flow and incoming flow in CtO configuration are in opposite direction, the superposition of the three component leads to the lowest velocity among other configurations. Although the major lift production area of both turbines is in the interaction zone, the constructive effect of this interaction does not give significant impact on turbines performance. The position of the major lift production area of CtO is depicted in Figure 3 (b). This is the main reason why CtO have the worst performance. Meanwhile, both induced flow of CtI configuration is in the direction of incoming flow, leading to the more powerful flow superposition, as shown in Figure 3 (c). This phenomenon results in an increase of energy potency in the interaction zone, which could significantly increase the lift production and both turbines performance.

Since the experimental result lacks in the detail of hydrodynamic interaction which arises around the turbines, the numerical simulation is needed to know exactly how this

interaction occurred. The hydrodynamics interaction could be distinguished easily by using the velocity contour got from the numerical simulation. The flow velocity in the interaction zone is in different value as each configuration has dissimilar induced flow, as illustrated in Figure 8. The red arrows represent the direction of induced flow and the blue one is for incoming flow. The CtI has the greatest velocity superposition and the CtO has the weakest. The velocity of interaction zone for Co, CtO and CtI are 1.4-1.6 m/s; 1.2-1.6 m/s and 1.6-1.8 m/s, respectively. The flow superposition is not the only reason for the flow acceleration in the interaction zone, the close distance between turbines also gives an important contribution. It raises channel effect or jet-type flow effect, resulting in the flow velocity enhancement. Both phenomena provide a constructive impact on turbines and array performance.

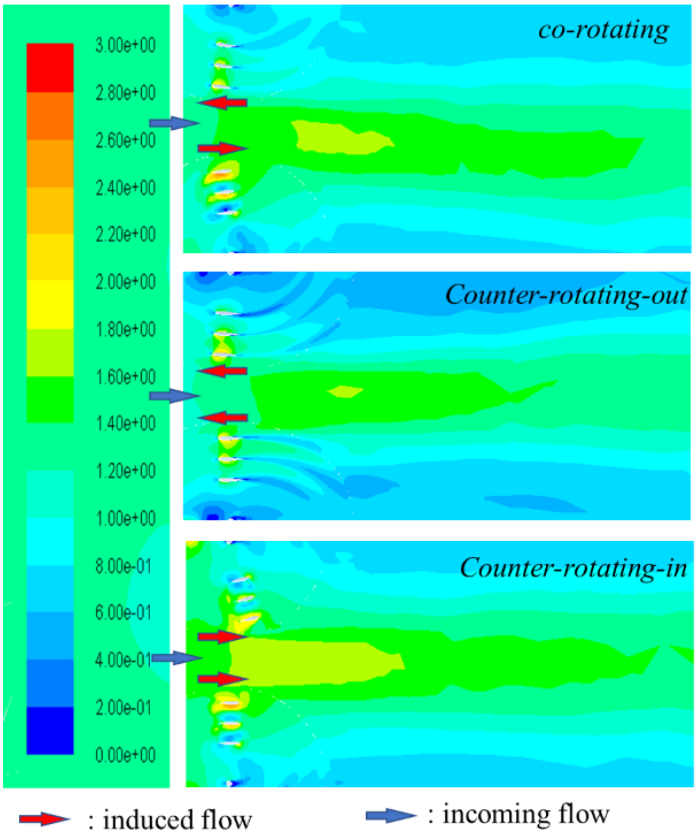

Figure 8. Velocity contour at interaction zone (in m/s)

To determine the flow velocity profile around the turbine, the velocity around the turbine is plotted in the cross stream (Y) and streamwise (X) direction, as shown in Figure 9. The turbine area is represented at Y/D= 0.25 – 1.5 (for turbine A) and Y/D= -0.25 - -1.5 (for turbine B), while Y / D = 0 represents the velocity profile in the center of the flow interaction zone. The flow fluctuation arises inside the turbine area. In contrast, the flow in the interaction zone seems to be more stable. At Y / D = 0; 0.25 and -0.25, it could be seen that the flow interaction in the CtI configuration has a greater induced velocity compared to others. Y / D = 0.25 and Y / D = -0.25 shows the side of the turbines which is directly related to the interaction zone, in which it has a more powerful hydrostatic interaction effect than the

other side. In this zone, the CtO configuration has the most fluctuate velocity. It indicates that if the induced flow and incoming flow is in opposite direction, the superposition of flow results in low velocity and greater flow fluctuation. The flow fluctuation is important to be considered as it causes more unstable hydrodynamic force, leading cause vibration and endanger the turbine structure

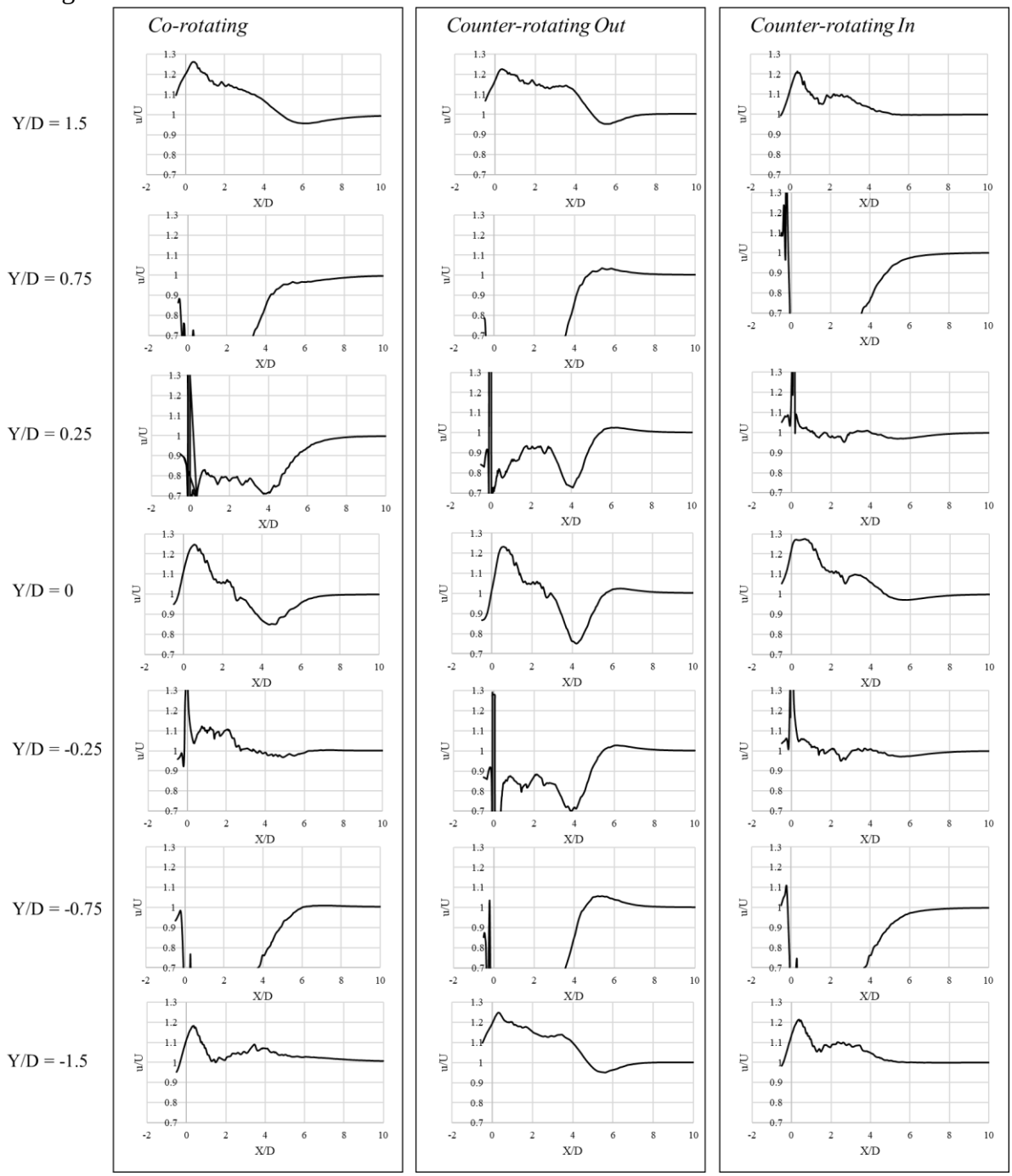

Figure 9. The plot of velocity fluctuation around the turbine

The flow characteristics around the turbine could also be analyzed through the characteristics of turbulence. In this case, the turbulent intensity parameter is employed as a quantity that shows turbulent conditions around the turbine. Turbulence could provide constructive and destructive effects on turbines. Incoming flow with weak turbulence could improve the performance of the turbines. However, stronger turbulence causes irregular flow and cause the turbine performance decrement [56].

Figure 10 shows the comparison of the turbulent intensity in the interaction zone for each configuration. The turbulent intensity is the ratio of velocity fluctuations and average flow velocities at a certain point. The characteristics of turbulent intensity around the turbine affect the flow quality, hence they greatly affect the performance of the turbines. A significant difference occurs in the CtI configuration, in which the induction flow is in the direction of the incoming flow, hence the flow is more stable. It has smaller turbulent intensity, confirming that the flow in the interaction zone tends to be more stable. As the CtI has faster velocity superposition and low turbulent intensity, its farm effectiveness tends to be greater than others.

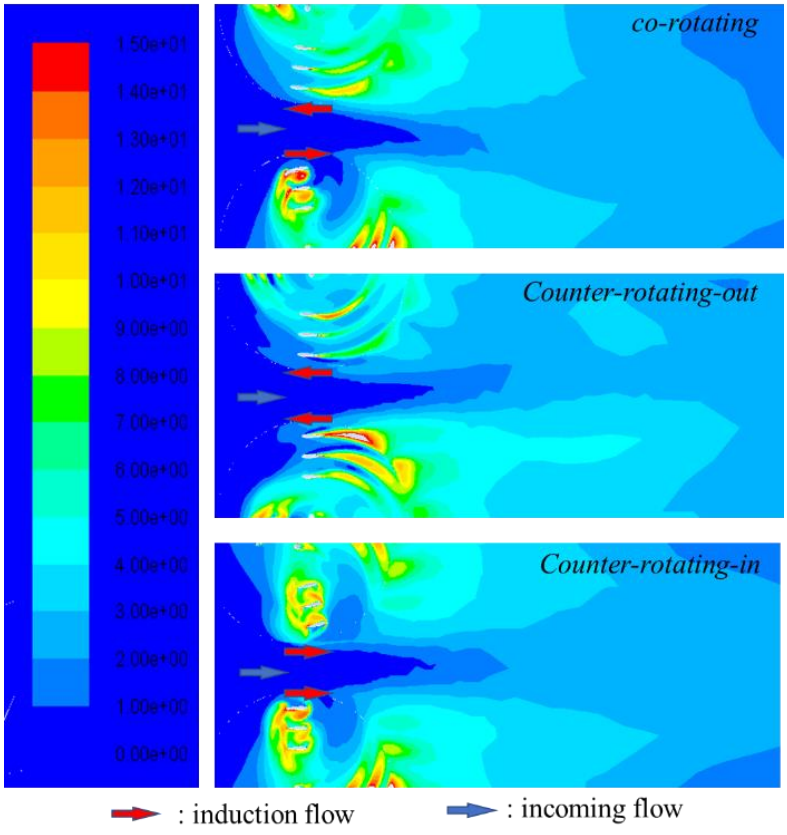

Figure 10. Contour of turbulent intensity at interaction zone (in %)

The significant difference of turbulent intensity does not occur in the interaction zone but inside the turbines. Figure 11 provides clear information of the turbulent intensity inside and around the turbine. The figures are the plot of the turbulent intensity which is taken at the center of the turbine along the cross-stream distance of -1 to 1 m (-2.5 to 2.5 D). The

turbulent intensity in the CtO configuration is greater than the others, which even reaches 25%. Meanwhile, the turbulent intensity for Co and CtI reaches 20% and 12.5%, respectively. The analysis of turbulent intensity establishes that the characteristics of hydrodynamics interaction influence the turbulent intensity characteristics.

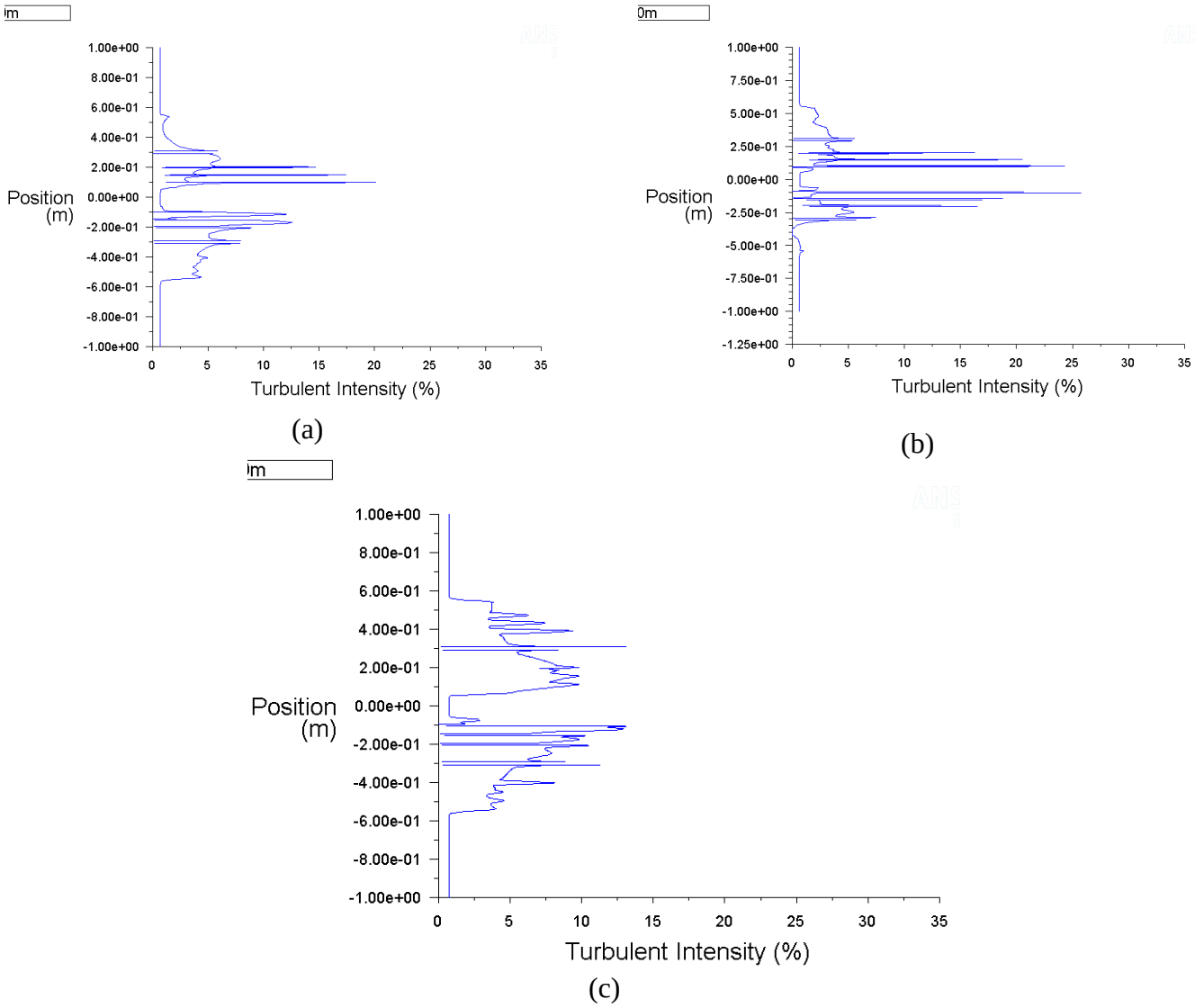

Figure 11. Plot of turbulent intensity fluctuation around the turbines for (a) Co configuration; (b) CtO configuration; (c) CtI configuration

Due to existent of flow separation, the turbulent intensity in the trailing edge is strong. Flow separation on the trailing edge leads to the formation of vortex structures. Vortex is indicated with rotating flow, which is usually represented by the vorticity magnitude. Vortex structure is an unstable flow and has a strong turbulent intensity. Vortices on the trailing edge cause the increment of turbulence along the path of the vortex, leading to greater turbulent intensity, as shown in Figure 12.

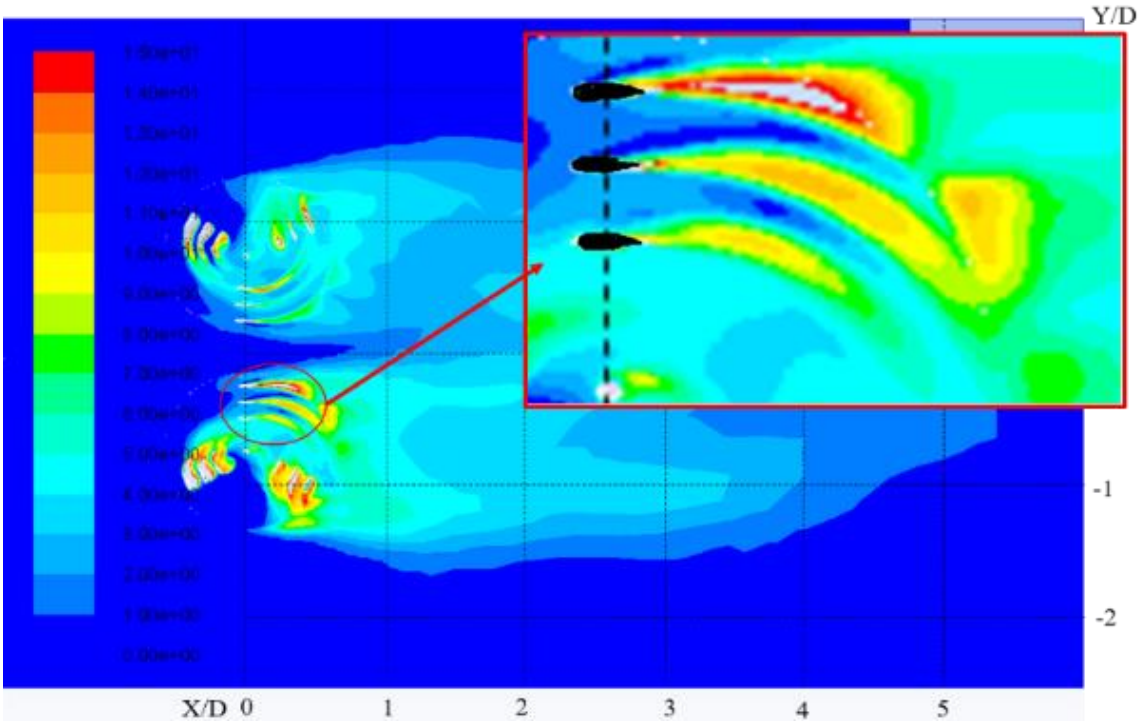

Figure 12. Detail of turbulent intensity near the trailing edge (in %)

Flow characteristics around vertical axis turbines are quite complex. The downstream blades and upstream blades are subjected by different flow characteristics. Due to the existence of upstream blade, the downstream part gets disturbed and unstable flow, which contains a lot of vortexes. The energy extraction process of the downstream blade makes it more complex. This causes differences in turbulent intensity in the upstream and downstream parts, in which the downstream part has greater turbulent intensity. In addition, there is a significant difference between turbulent intensity in the major lift production zone and minor lift production zone. The former tends to have higher turbulent intensity than the latter.

Turbulent formed as the turbine rotate is a weak turbulent, which is easy to dissipate. Turbulent requires a sustainable energy supply to overcome losses due to the effect of fluid viscosity. If no energy is supplied, turbulence will quickly disappear or be dissipated [57]. In the case, turbine movement forms many vortex structures and supply the energy requirements to keep the turbulence. Therefore, turbulent flow in the turbine area exists as long as the turbine rotates. This turbulence propagates to the downstream zone (propagating towards the x-axis), thus the turbulence intensity in that area is higher than inlet. Moreover, the downstream zone has many vortex structures, which are formed due to energy extraction by the turbine. Thus, its velocity is unstable. However, the effect of turbulent intensity increment is not too far away. The turbulence will be quickly dissipated as it moves beyond the turbine. Meanwhile, the propagation of turbulence to the side of the turbine is not widespread (propagation to the y-axis). Turbulence that propagates to the side of the turbine is more easily dissipated than turbulence, which moves to the downstream area. Thus, the turbulent intensity in the interaction zone has the lower value. Despite the turbine rotational direction does not have a significant impact on turbulent intensity in the interaction zone, it has a powerful impact on the turbulent intensity inside the turbine.

Hydrokinetic turbine is applicable to various site conditions, either site which has uniform flow direction or that which has changeable direction. CtI configuration is more recommended for sites with a uniform flow direction, since it performs better. However, this not recommended for application in site with changeable flow direction, as CtI would change to the CtO configuration and cause a difference in hydrodynamics interactions when the direction of the current is opposite to the direction of the previous current. This actually causes a significant performance reduction. Therefore, the Co configuration is more recommended for sites with the changeable flow direction.

Performance of Multi-row Configuration

Array installation in a single row is less effective when applied to a wide site. In order to meet the energy production target, the turbine array is arranged in several rows (consisting of upstream and downstream turbines). This study analyzed the effect of adding a turbine in front of or rear of side-by-side configuration. Experimental results and simulations for the side-by-side configuration were taken into consideration in designing multi-row configuration. It was mentioned earlier that the Co and CtI configurations have almost the same farm effectiveness, hence multi-row configuration employs Co Configuration. This study proposed two different multi-row array configurations, knowns as 3TA and 3TB.

The weakness of multi-row installation is the performance of a downstream turbine which is not optimal, as it works on the wake of upstream turbine. Downstream turbines actually have to be installed beyond the wake area. Thus, the adverse effects of wake could be avoided. However, with the limited of installation area, the downstream turbine is still installed in the far wake region. To reduce the adverse effect of wake, the turbine is installed in zig-zag configuration, as in the 3T-A and 3T-B configurations.

The experimental result confirmed that the performance of 3T-A is better than the 3T-B, given at Figure 13. 3T-A perform better although at the low incoming flow velocity, i.e. 0.7 m/s, with the farm effectiveness approximately 1.075. Meanwhile, at the same incoming flow velocity, 3-TA only reach 0.93.

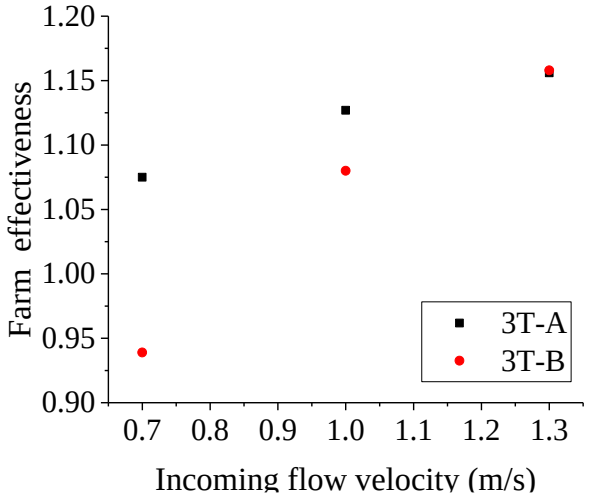

Figure 13. Performance of multi-row configuration

Turbines A and B have a greater Cp than stand-alone turbines, as illustrated in Figure 14 (a). The numerical simulation was carried out to observe this phenomenon. Its result is given in Figure 15. The constructive interaction between side-by-side turbines seems to be very influential in this phenomenon. Beside the superposition of induced flow and incoming flow which result in performance improvement, the interaction of these two turbines will cause a channel effect that results in flow acceleration in the interaction zone, as shown in Figure 15 (a). In addition, this causes the velocity vector to be more directed, which is usually indicated by a low vorticity value. The constructive effects of installing side-by-side downstream turbine arrays are able to compensate for the destructive effects of the upstream turbine wake. Thus, downstream turbines continue to experience performance improvements, even more than stand-alone turbines.

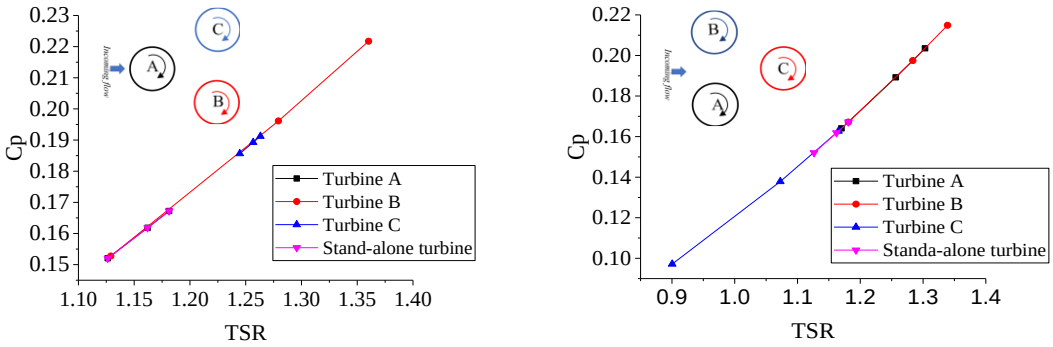

Figure 14. Performance of each turbine in multi-row configuration for: (a) 3TA configuration; (b) 3TB configuration

Different phenomena appear in the 3T-B configuration. Downstream turbine (Turbine C) is subjected by the wake of upstream turbines, as shown in Figure 15 (b). Hence, the adverse effect of wake toward the downstream turbine in 3T-B is more powerful than that for the 3T-A. In 3T-B, the downstream turbine operates alone (not in the side-by-side configuration), so that the constructive effects of hydrodynamic interactions do not take place, thus the 3T-B configuration to have a worse performance than 3T-A.

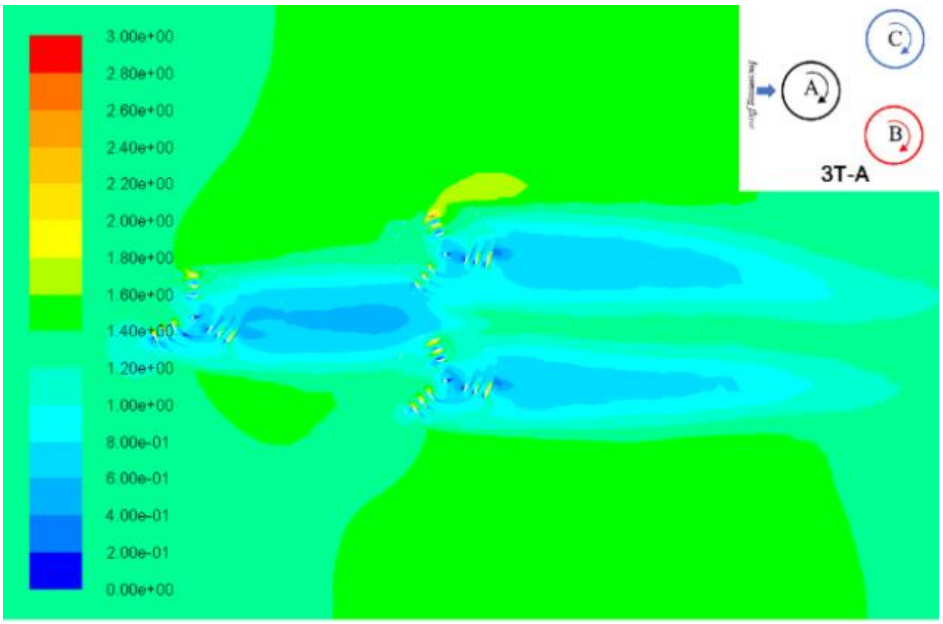

(a)

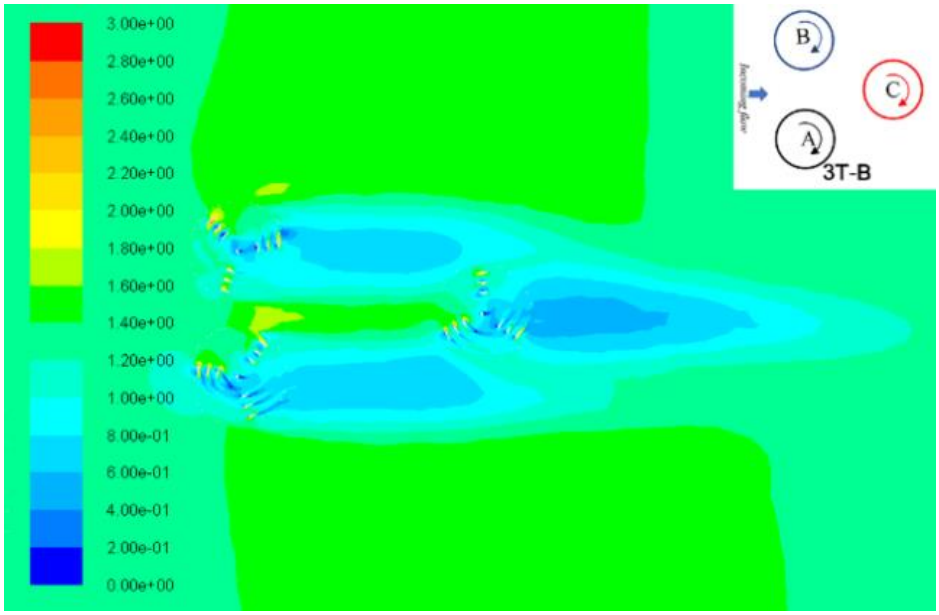

(b)

Figure 15. Velocity contour of multi-row configuration for: (a) 3TA configuration; (b) 3TB configuration

The experimental results and numerical simulations confirmed that the phenomena occurred in the three-turbine configuration supports that the installation of two turbines in side-by-side configuration provides a significant performance improvement. Even this performance improvement is able to compensate the adverse effects of the upstream turbines wake.

CONCLUSIONS

This research pursues the previous research regarding to the novel design on Vertical Axis Hydrokinetic Turbine-Straight Blade Cascaded (VAHT-SBC) and its array configuration. Experimental and numerical study was carried out and confirmed that the hydrodynamic interaction which is occurred could improve the performance of each turbine, leading to farm effectiveness improvement. Due to different turbines' rotational direction, the different hydrodynamic interaction raised, causing different value of velocity and turbulent intensity contour. Velocity superposition in the interaction zone depends on the direction of induced velocity which hinge on turbine rotational direction.

Since both induced velocity of CtI is in the same direction with incoming flow, the velocity superposition of Ctl seem to have more constructive effect than others, which is indicated by high farm effectiveness for all velocity variation. The farm effectiveness for Co and CtI reach 1.33 and 1.37, respectively. The installation of site by site configuration leading provides a performance improvement of more than 30% at incoming flow of 1.3 m/s.

Installation of site-by-site configuration as downstream turbines on multi-row configurations is able to compensate for the adverse effects of upstream turbine wake, hence downstream turbine performance increases, even higher than stand-alone turbine. This phenomenon is the reason why the farm effectiveness of 3T-A more than 1, even for low incoming flow velocity. However, the downstream turbine of 3T-B is not site-by-site configuration, till it could not pay off the adverse effect of upstream turbines' wake.

REFERENCE

[1] Gonzalo T, Claudio T, Federico Z. Numerical analysis of a diffuser-augmented hydrokinetic turbine. Ocean Engineering. 2017; 145:138-47

[2] Outlook Energy. BPPT- Outlook Energi Indonesia 2017. 2017.

[3] Lucas IL, Fernando LP, Lin-Fan C. Advances and trends in hydrokinetic turbine systems, Energy Sustainable Development. 2010; 14:287-96

[4] Stefania Z, Ferdinando B, Niccolo B. Hydrodynamic interactions between three closely spaced vertical axis tidal turbines. Energy Procedia. 2016; 101: 520–27

[5] In SH, Yun HL, Seung JK. Optimization of cycloidal water turbine and the performance improvement by individual blade control. Applied Energy. 2009; 86:1532–40

[6] Maarten C. The design and testing of airfoils for application in small vertical axis wind turbines. TUDelft. 2006.

[7] Wirachai R. Optimisation of vertical axis wind turbines. Northumbria University. 2004

[8] Brian K. Tests on ducted and bare helical and straight blade Darrieus hydrokinetic turbines. Renewable Energy. 2011; 36: 3013–22.

[9] Frank S, Timothy MF, Richard EB. The influence of blade curvature and helical blade twist on the performance of a vertical-axis wind turbine. In: 29th ASME Wind Energy Symposium, 2010; 1–16.

[10] Mark HW. Aerodynamic performance of the 17 meter diameter Darrieus wind turbine. Journal Energy. 1981;5:39-42

[11] Marco RC. Effect of Blade Inclination Angle on a Darrieus Wind Turbine. Journal of Turbomachinery. 2017; 134: 1–10.
[12] Ridho H, Erna S. Novel Design of a Vertical Axis Hydrokinetic Turbine –Straight-Blade Cascaded (VAHT–SBC): Experimental and Numerical Simulation. Journal of Engineering Technology and Science. 2018; 50: 73–86
[13] Ridho H, I Ketut APU, Erwandi, Aries S. An experimental investigation of passive variable-pitch vertical-axis ocean current turbine. Journal of Engineering Technology and Science. 2011; 43: 27–40.
[14] Ridho H, Juniarko P, Ahmad WM, Erna S, Fahmi I. Performance investigation of an innovative Vertical Axis Hydrokinetic Turbine – Straight Blade Cascaded (VAHT-SBC) for low current speed Performance investigation of an innovative Vertical Axis Hydrokinetic Turbine – Straight Blade Cascaded (VAHT- SBC). Journal of Physics: Conference Series. 2018; 1022
[15] Ridho H, I Ketut APU, Irfan SA, Abdi I, Seno WM. Innovation in Vertical Axis Hydrokinetic Turbine – Straight Blade Cascaded (VAHT-SBC) design and testing for low current speed power generation Innovation in Vertical Axis Hydrokinetic Turbine – Straight Blade Cascaded (VAHT-SBC) design and testing for low current speed power generation. 2018. Journal of Physics: Conference Series. 2018; 1022
[16] Martin N, Longbin T. Experimental study of wake characteristics in tidal turbine arrays. Renewable Energy.2018; 127: 168–81.
[17] Nicholas DL, Brenden PE. Hydrokinetic energy conversion: Technology, research, and outlook. Renewable and Sustainable Energy Review. 2016; 57: 1245–59.
[18] Saurabh C, Craig H, Xiaolei Y, Michele G, Dean C, Jonathan C, Fotis S. Wake characteristics of a TriFrame of axial-flow hydrokinetic turbines. Renewable Energy. 2017; 109: 332–45.
[19] Stephanie OS, Duncan S, Gregory SP, Tom B, Mulualem G, Michael RB, Ian M. Experimental evaluation of the wake characteristics of cross flow turbine arrays. Ocean Engineering. 2017; 141: 215–26.
[20] Penny J, Trevor W, Cuan B, Bjoern E. Field tests of multiple 1 / 10 scale tidal turbines in steady flows. Renewable Energy.2016; 87: 240–52.
[21] Harrison ME, Batten WMJ, Myers LE, Bahaj AS. A comparison between CFD simulations and experiments for predicting the far wake of horizontal axis tidal turbines. Renewable Power Generation.2010; 4: 613–27.
[22] Scott D, Guy TH, M. L. G. Oldfield, Alistair GLB. Modelling Tidal Energy Extraction in a Depth-Averaged Coastal Domain. 2010; 4: 1045–52.
[23] Thomas AAA, Scott D, Guy TH, Alistair GLB, Sena S. The available power from tidal stream turbines in the Pentland Firth. Proceedings of The Royal Society A (Mathematical, Physical and Engineering Sciences). 2013; 469: 1-21
[24] Alex O, Tim S, Tong F, Peter KS. Comparison of a RANS blade element model for tidal turbine arrays with laboratory scale measurements of wake velocity and rotor thrust. Journal of Fluids Structure.2016; 64: 87–106.
[25] Robert JC. Wind turbine and sodar observations of wakes in a large wind farm. in 19th Symposium on Boundary Layers and Turbulence. 2010.
[26] Wei Y, Ahmed O, Wei T, Hui H. An Experimental Investigation on the Effect ofTurbine Rotation Direction on the Wake Interference of Wind Turbine, in Aiaa. 2013; 3815: 1–18.

[27] Nak JL, In CK, Chang GK, Beom SH, Young HL. Performance study on a counter-rotating tidal current turbine by CFD and model experimentation. Renewable Energy.2015; 79: 122–26.

[28] Michael B, Andrew S, Maurizio C. Offshore floating vertical axis wind turbines, dynamics modelling state of the art. part I: Aerodynamics. Renewable Sustaintainable Energy Review. 2014; 39: 1214–25.

[29] Carlos SF, Helge AM, Metthew B, Bjorn R, P. Deglaire, I. Arduin. Comparison of aerodynamic models for Vertical Axis Wind Turbines. Journal of Physics: Conference Series. 2014; 524.

[30] Tescione G, Carlos JSF, Gerard JWVB. Analysis of a free vortex wake model for the study of the rotor and near wake flow of a vertical axis wind turbine. Renewable Energy. 2016; 87: 552–63.

[31] Nobuyuki F, Satoshi S. Observations of dynamic stall on Darrieus wind turbine blades. Journal of Wind Engineering and Industrial Aerodynamic. 2001; 89: 201–214.

[32] Mojtaba AB, Rupp C, David SKT. A wind tunnel study on the aerodynamic interaction of vertical axis wind turbines in array configurations. Renewable Energy. 2016; 96: 904–913.

[33] Ian R, Aaron A. Wind Tunnel Blockage Corrections: Review and application to Savonius Vertical-Axis Wind Turbines. Journal of Wind Engineering and Industrial Aerodynamic. 2011; 99: 523–38.

[34] Ross V. Tuning tidal turbines in-concert to maximise farm efficiency. Journal of Fluid Mechanics. 2011; 671: 587–604.

[35] Ye L. On the definition of the power coefficient of tidal current turbines and efficiency of tidal current turbine farms. Renewable Energy. 2014; 68: 868–75.

[36] Yoshihide T, Ted S. Steady and unsteady RANS simulations of pollutant dispersion around isolated cubical buildings: Effect of large-scale fluctuations on the concentration field. Journal of Wind Engineering and Industrial Aerodynamic. 2017; 165: 23–33.

[37] Kato M, Brian L. The modeling of turbulent flow around stationary and vibrating square cylinders. Ninth Symp. Turbul. Shear Flows. 1993; 10.4.1-10.4.6.

[38] Wolfgang R. On the simulation of turbulent flow past bluff bodies. Journal of Wind Engineering and Industrial Aerodynamic. 2993; 46: 3–19.

[39] Shuzo M, Akashi M, Yoshihiki H, Shigehiro S. Numerical study on velocity-pressure field and wind forces for bluff bodies by k-ε, ASM and LES. Journal of Wind Engineering and Industrial Aerodynamic. 1992; 44: 2841–52.

[40] Claudio M, Ante Š, Ralph Voß, Gunter S. Unsteady RANS simulations of flow around a bridge section. Journal of Wind Engineering and Industrial Aerodynamic. 2010; 98: 742–53.

[41] Claudio M, Ante Š, Gunter S. Unsteady RANS modelling of flow past a rectangular cylinder: Investigation of Reynolds number effects. Computational Fluids. 2010; 39: 1609–24.

[42] Alberto P, Craig M. Vortex shedding from a wind turbine blade section at high angles of attack. Journal of Wind Engineering and Industrial Aerodynamic. 2013; 121: 131–37.

[43] Salim MS, Kian CO. Performance of RANS, URANS and LES in the prediction of airflow and pollutant dispersion. Lecture Notes in Electrical Engineering. 2013; 170: 263–74.
[44] Florian RM. Two-equation eddy-viscosity turbulence models for engineering applications. AIAA Journal. 1994; 32: 1598–605.
[45] Philip M, Dev R, Irene P, Giles T. Numerical investigation of the influence of blade helicity on the performance characteristics of vertical axis tidal turbines. Renewable Energy. 2015; 81: 926–35.
[46] Brian KK, Leo L. Limitations of fixed pitch Darrieus hydrokinetic turbines and the challenge of variable pitch. Renewable Energy. 2011; 36: 893–97.
[47] Bo Y, Chris L. Fluid dynamic performance of a vertical axis turbine for tidal currents. Renewable Energy. 2011; 36: 3355–66.
[48] Hendrik KV, Weeratunge M. An introduction to computational fluid dynamics. 2007.
[49] Florian RM. Zonal Two Equation k-ω Turbulence Models for Aerodynamic Flows. in 24th Fluid Dynamics Conference. 1993.
[50] Paulo ACR, Helio HBR, F. O. M. Carneiro, Maria EVS, Carla FA. A case study on the calibration of the k-ω SST (shear stress transport) turbulence model for small scale wind turbines designed with cambered and symmetrical airfoils. Energy. 2016; 97: 144–50.
[51] Muhammad SS, Adil R, Trond K, Mandar T. Effect of turbulence intensity on the performance of an offshore vertical axis wind turbine. Energy Procedia. 2015; 80: 312–20.
[52] Guang Z, Ran SY, Yan L, Peng FZ. Hydrodynamic performance of a vertical-axis tidal-current turbine with different preset angles of attack. Journal of Hydrodynamic. 2013; 25: 280–87.
[53] Antonio P, Colin MP, Megan CL, Elias B. Wake structure of a single vertical axis wind turbine. International Journal of Heat and Fluid Flow. 2016: 61; 75–84.
[54] Abdolrahim R, Ivo K, Bert B. CFD simulation of a vertical axis wind turbine operating at a moderate tip speed ratio: Guidelines for minimum domain size and azimuthal increment. Renewable Energy. 2017: 107; 373–85.
[55] John OD. Potential order of magnitude enhancement of wind farm power density via counter-rotating vertical-axis wind turbine arrays. Journal of Renewable and Sustainable Energy. 2011; 3: 043-104.
[56] Kristine M. Effect of free stream turbulence on wind turbine performance. 2013.
[57] Henk T, John L. A first course in turbulence. Cambridge, Massachusetts, London: MIT Press.